Transition Metal Coordinated $Al(X)L_2$ and $Ga(X)L_2$ Fragments†

Roland A. Fischer,*,‡,§ Markus M. Schulte,§ Jurij Weiss,§ Laszlo Zsolnai,§ Albrecht Jacobi,§ Gottfried Huttner,§,⊥ Gernot Frenking,*,||,▽ Christian Boehme,▽ and Sergei F. Vyboishchikov▽

Contribution from the Ruprecht-Karls-Universtiät Heidelberg, Im Neuenheimer Feld 270, D-69120 Heidelberg, Germany, and Fachbereich Chemie, Philipps-Universität Marburg, Hans-Meerwein-Strasse, D-35032 Marburg, Germany

Received May 20, 1997

Abstract: Carbonylmetalate dianions react in thf with the group 13 chlorides X_mECl_{3-m} (E = Al, Ga; X = Cl, Me, Et, ^{i}Bu; m = 0, 1) to yield the monoanionic species $[(CO)_nM-EX_mCl_{2-m}]^-$ (M = Fe, Cr, Mo, W; n = 4, 5) as the primary products which could be isolated as solvent free salts after exchange with a non coordinating cation. After addition of a chelating Lewis base, e.g., tmeda, dme, and solvent exchange with dichloromethane the primary products undergo a second salt elimination reaction, yielding the neutral intermetallic systems $(CO)_nM-Ga[X(L)_2]$ (M = Cr, Mo, W, Fe; n = 4, 5; X = Cl, Me, Et; L_2 = tmeda, dme, bipy, ^{t}Bu-dab, thf_2) (**1**−**14**) and $(CO)_5M-Al[X(L)_2]$ (M = Cr, Mo, W; X = Cl, Et, ^{i}Bu; L_2 = tmeda, tmpda) (**15**−**20**, **23**, **24**). The chloro derivatives can be converted to the corresponding hydrido or tetrahydridoboranato species which is exemplarily shown by compounds **21** and **22**. In the case of R_2GaCl (R = Me, Et; 2 equiv) as starting compounds a ligand exchange reaction, generating GaR_3, occurs, before the second salt elimination takes place. The new intermetallic systems were characterized by means of elemental analysis and IR, Raman, NMR, and mass spectroscopy. The complexes $(CO)_5Cr-Ga[Cl(tmeda)]$ (**2**), $(CO)_5W-Al[Et(tmeda)]$ (**20**), and $(CO)_5W-Al[Cl(tmpda)]$ (**23**) are also characterized by single-crystal X-ray diffraction. Compounds **2** and **20** crystallize in the monoclinic space group $P2_1/n$, Z = 4. **2**: a = 9.059(4) Å, b = 16.084(7) Å, c = 11.835(6) Å, β = 80.6(1)°, V = 1701(1) Å^3, and R = 0.037 (R_w = 0.118). **20**: a = 8.606(2) Å, b = 16.463-(6) Å, c = 12.469(4) Å, β = 93.88(2)°, V = 1762(6) Å^3, and R = 0.027 (R_w = 0.065). Complex **23** crystallizes in the orthorhombic space group *Pccn*, a = 23.990(6) Å, b = 9.044(3) Å, c = 15.871(4) Å, V = 3445(1) Å^3, and R = 0.044 (R_w = 0.088). Ab initio quantum chemical calculations at the MP2 level of theory of the model complexes $(CO)_5W-E[Cl(NH_3)_2]$ (E = B, Al, Ga, In, Tl), $(CO)_5W-Al[H(NH_3)_2]$, $(CO)_5W-AlH$, and $(CO)_5W-AlCl$ are reported. The group-13 fragments $E(R)L_2$ behave as strong σ-donors with significant acceptor capabilities. The W−E bonds are strong semipolar covalent bonds with large ionic contributions (D_e(calc) between 70 and 120 kcal/mol). Only the W−Tl bond is comparatively weak (D_e(calc) = 48 kcal/mol).

Introduction

The chemistry of subvalent halides and organometallic compounds of aluminum and gallium is currently flourishing. This wide interest originates not only from theoretical points of view with respect to structure and bonding but also from preparative challenges and new opportunities using these compounds as synthetic starting materials.[1] Prominent examples include the fascinating tetrahedral compound $[Cp^*Al]_4$,[2] its alkyl congeners $(RE)_4$ and $R'_2E-ER'_2$ (R = TMS_2CH; R′ = TMS_3C; E = Al, Ga, In),[3,4] and multiple bonded anionic species such as $[R_2Al-AlR_2]^-$.[4] Recently we communicated the synthesis, structure, and bonding of $[(\eta^5\text{-}C_5Me_5)Al-Fe(CO)_4]$, the first example of a compound with a Cp*Al unit strongly bonded to a transition metal fragment in a terminal nonbridging fashion.[5a] Particularly noteworthy here is the very recent report of G. H. Robinson et al. on the complex $(CO)_4Fe-Ga(C_6H_3Mes^*_2)$ (Mes* = 2,4,6-$^i Pr_3C_3H_2$), which was discussed as the first example of a ferrogallyne with a Fe−Ga triple bond.[5b] We also have demonstrated the potential of a Lewis base adduct stabilized congener $(CO)_5Cr-Ga[(Et)(tmeda)]$ as volatile single source precursors to deposit stoichiometric intermetallic CrGa thin films by using organometallic chemical vapor deposition.[6] Interestingly, the metal−metal bonded single source precursors with monoalkyl ER units rather than dialkyl fragments ER_2[7−9] proved to be advantageous with respect to achieving perfect

† Organo Group 13 Transition Metal Complexes. 16. Part 15: see ref 36.
‡ E-mail: roland.fischer@urz.uni-heidelberg.de.
§ Ruprecht-Karls-Universität Heidelberg. Note the new address of R.A.F. and J.W.: Ruhr-Universität Bochum, Lehrstuhl für Anorganische Chemie II, D-44780 Bochum, Germany.
⊥ X-ray Crystallography.
|| E-mail: frenking@ps1515.chemie.uni-marburg.de.
▽ Philipps-Universität Marburg.

(1) Dohmeier, C.; Loos, D.; Schnöckel, H. *Angew. Chem.* **1996**, *108*, 141−161; *Angew. Chem., Int. Ed. Engl.* **1996**, *35*, 129−149.
(2) Dohmeier, C.; Robl, C.; Tacke, M.; Schnöckel, H. *Angew. Chem.* **1991**, *103*, 594−595; *Angew. Chem., Int. Ed. Engl.* **1991**, *30*, 564−565.
(3) Uhl, W. *Angew. Chem.* **1993**, *105*, 1449−1461; *Angew. Chem., Int. Ed. Engl.* **1993**, *32*, 1386-1398.
(4) Wehmschulte, R. J.; Ruhland-Senge, K.; Olmstead, M. M.; Hope, H.; Sturgeon, B. E.; Power, P. P. *Inorg. Chem.* **1993**, *32*, 2983−2984.
(5) (a) Weiss, J.; Stetzkamp, D.; Nuber, B.; Fischer, R. A.; Boehme, C.; Frenking, G. *Angew. Chem.* **1997**, *109*, 95−97; *Angew. Chem., Int. Ed. Engl.* **1997**, *36*, 70−72. (b) Su, J.; Li, X.-W.; Crittendon, R. C.; Campara, F. C.; Robinson, G. H, *Organometallics* **1997**, *16*, 4511−4513.
(6) Schulte, M. M.; Herdtweck, E.; Raudaschl-Sieber, G.; Fischer, R. A. *Angew. Chem.* **1996**, *108*, 489−491; *Angew. Chem., Int. Ed. Engl.* **1996**, *35*, 424−426.
(7) Fischer, R. A.; Miehr, A.; Priermeier, T. *Chem. Ber.* **1995**, *128*, 831−843.
(8) (a) Fischer, R. A.; Priermeier, T. *Organometallics* **1994**, *13*, 4306−4314. (b) Braunschweig, H.; Müller, J.; Gaufer, B. *Inorg. Chem.* **1996**, *35*, 7443−7444. (c) Anand, B. N.; Krossing, I.; Nöth, H. *Ibid.* **1997**, *36*, 1979−1981.
(9) Fischer, R. A.; Herdtweck, E.; Priermeier, T. *Inorg. Chem.* **1994**, *33*, 934−943.

S0002-7863(97)01646-6 CCC: $15.00
Published on Web 02/03/1998

Table 1. Infrared ν(CO) Data of the New Complexes **1**−**24**

compound	no.	ν(CO)
	New Compounds[a]	
$(CO)_5Cr-Al[(Cl)(tmeda)]$	**15**	2016 (s), 1926 (vs), 1876 (vs)
$(CO)_5Cr-Al[(CH_2CH_3)(tmeda)]$	**16**	2001 (vs), 1936 (vs), 1870 (vs, br)
$(CO)_5Mo-Al[(Cl)(tmeda)]$	**17**	2031 (m), 1937 (vs), 1887 (vs)
$(CO)_5Mo-Al[(CH_2CH_3)(tmeda)]$	**18**	2018 (s), 1934 (vs), 1879 (vs)
$(CO)_5W-Al[(Cl)(tmeda)]$	**19**	2031 (m), 1933 (vs, br), 1885 (vs, br)
$(CO)_5W-Al[(Cl)(tmpda)]$	**23**	2030 (m), 1934 (s, sh), 1888 (vs, br)
$(CO)_5W-Al[(CH_2CH_3)(tmeda)]$	**20**	2018 (s), 1933 (vs), 1876 (vs)
$(CO)_5W-Al[(^iBu)(tmpda)]$	**24**	2019 (m), 1934 (vs), 1877 (vs)
$(CO)_5Cr-Ga[(Cl)(thf)_2]$	**1**	2039 (m), 1955 (w, sh), 1913 (vs)
$(CO)_5Cr-Ga[(Cl)(tmeda)]$	**2**	2033 (vs), 1947 (s), 1900 (vs)
$(CO)_5Cr-Ga[(Cl)(dme)]$	**3**	2040 (m), 1956 (m, sh), 1913 (s)
$(CO)_5Cr-Ga[(Cl)(bipy)]$	**4**	2030 (s), 1942 (m, sh), 1902 (vs)
$(CO)_5Cr-Ga[(Cl)(tBu-dab)]$	**5**	2034 (s), 1947 (m), 1919 (vs), 1885 (vs, sh)
$(CO)_5Cr-Ga[(H)(tmeda)]$	**21**	2012 (m), 1933 (s, sh), 1883 (vs)
$(CO)_5Cr-Ga[(BH_4)(tmeda)]$	**22**	2020 (m), 1923 (m, sh), 1905 (m, sh), 1885 (vs)
$(CO)_5Cr-Ga[(Me)(tmeda)]$	**6**	1992 (vs), 1905 (s), 1863 (vs)
$(CO)_5Cr-Ga[(CH_2CH_3)(tmeda)]$	**7**	2012 (ms), 1918 (w,sh), 1882 (vs)
$(CO)_5Mo-Ga[(Cl)(tmeda)]$	**8**	2050 (vs), 1963 (s, sh), 1914 (vs)
$(CO)_5Mo-Ga[(CH_2CH_3)(tmeda)]$	**9**	2030 (s), 1938 (s), 1900 (vs)
$(CO)_5W-Ga[(Cl)(tmeda)]$	**10**	2048 (vs), 1956 (s), 1917 (vs)
$(CO)_5W-Ga[(CH_2CH_3)(tmeda)]$	**11**	2030 (vs), 1932 (vs), 1892 (vs)
$(CO)_4Fe-Ga[(Cl)(tmeda)]$	**12**	2011 (vs), 1928 (vs), 1881 (vs)
$(CO)_4Fe-Ga[(CH_3)(tmeda)]$	**13**	1992 (vs), 1905 (s), 1863 (vs)
$(CO)_4Fe-Ga[(CH_2CH_3)(tmeda)]$	**14**	1992 (vs), 1905 (s), 1863 (vs)
	Reference Compounds[b−d]	
$(CO)_5Cr-Si[o-(Me_2NCH_2)C_6H_4]_2$		2036 (m), 1916 (vs), 1884 (vs)[b]
$(CO)_5Cr-Si[(O^tBu)_2(hmpt)]$		2015 (m), 1991 (vs), 1930 (vs)[c]
$(CO)_4Fe-Si[(O^tBu)_2(hmpt)]$		2005 (w), 1920 (s), 1883 (vs)[c]
$(CO)_4Fe-P(NMe_2)_3$		2053 (w), 1975 (s), 1937 (vs)[d]

[a] All ν(CO)-IR data were obtained in CH_2Cl_2 solution between CaF_2 plates. [b] Data taken from Probst, R.; Leis, Ch.; Gamper, S.; Herdtweck, E.; Zybill, C.; Auner, N. *Angew. Chem., Int Ed. Engl.* **1991**, *30*, 1132−1134. [c] Data taken from Leis, C.; Wilkinson, B. L.; Handwerker, H.; Zybill, C.; Müller, G. *Organometallics* **1992**, *11*, 514−529. [d] Data taken from Hsieh, A. T. T.; Mays, M. J.; Platt, R. H. *J. Chem. Soc. A* **1971**, 3296−2302.

molecular control of the thin film stoichiometry.[6,10−13] We were thus led to investigate in more detail the synthesis, chemistry, structure, and bonding of AlX and GaX fragments bonded to transition metals in compounds of the general formula $(CO)_nM-E[(X)L_2]$ (M = Cr, Mo, W, n = 5; M = Fe, n = 4; E = Al, Ga; X = Cl, alkyl; $L_2 = Me_2N(CH_2)_mNMe_2$, m = 2, 3, or L = thf, NMe_3). Ab initio quantum chemical calculations at the MP2 level of theory of the model complexes $(CO)_5W-E[Cl(NH_3)_2]$ (E = B, Al, Ga, In, Tl), $(CO)_5W-Al[H(NH_3)_2]$, $(CO)_5W-AlH$, and $(CO)_5W-AlCl$ are reported. To gain insight into the M−E bonding situation of the molecules, we analyzed the electronic structure using the natural bond orbital (NBO) method developed by Weinhold[14] and the topological analysis of the electron density distribution developed by Bader.[15] We also characterized the metal−ligand interactions with the help of the newly developed charge-decomposition analysis (CDA).[16]

Experimental Section

Materials and Methods. All manipulations were undertaken utilizing standard Schlenk and glovebox techniques under inert gas atmospheres (purified N_2 or argon). Solvents were dried under N_2 by standard methods and stored over molecular sieves (4 Å, Merck; residual water <3 ppm, Karl Fischer). Infrared spectra were recorded as solutions between CaF_2 plates with a Perkin-Elmer 1600 FT-IR instrument and are reported in reciprocal centimeters. JEOL JNM-GX400, JNM-GX270, and BRUKER EM 200 spectrometers were used for NMR spectroscopy (^{1}H and ^{13}C NMR spectra were referenced to internal solvent and corrected to TMS).[27] Al NMR spectra were referenced to external standard $[Al(H_2O)_6]^{3+}$ (δ = 0). ^{11}B NMR spectra were referenced to diluted 10% H_3BO_3 (δ = 0) as external standard. All samples for NMR spectra were contained in vacuum-sealed NMR tubes. Melting points were observed in sealed capillaries and were not corrected. Raman spectra were recorded on a Riber Jobin Yvon Intruments S. A. spectrometer joint with a Coherent Innova 301 Krypton laser unit as a CH_2Cl_2 solution in quartz cuvettes or directly from single crystals. Starting compounds Cl_2GaEt, Cl_2GaMe, $ClGaMe_2$,[17] $K_2[Fe(CO)_4]$,[18] and $K_2[Cr(CO)_5]$[19] were prepared as discribed in the literature. $GaCl_3$ and Cl_2AlEt were used without further purification as purchased from HERAEUS and Aldrich; $AlCl_3$ was purchased from Aldrich, dried, and purified by sublimation. Abbreviations are as follows: Me = CH_3, Et = CH_2CH_3, ^{t}Bu = *tert*-butyl, Ph = phenyl, tmeda = *N*,*N*,*N*′,*N*′-tetramethylethylenediamin, tmpda = *N*,*N*,*N*′,*N*′-tetramethylpropylenediamine, dme = 1,2-dimethoxyethane, bipy = 2,2′-bipyridine, ^{t}Bu-dab = 1,4-di-tert-butyl-1,4-diazabuta-1,3-diene. Elemental analyses were provided by the Microanalytic Laboratory of the Technical University at Munich and the University of Heidelberg. Selected spectroscopic and analytical data of the new compounds are compiled in Tables 1−5.

Preparation of $K_2[Mo(CO)_5]$ and $K_2[W(CO)_5]$. According to the published preparation of $K_2[Cr(CO)_5]$,[19] the pentacarbonylmetalate dianions of molybdenum and tungsten are prepared in situ from the reduction of the hexacarbonyls with potassium graphite KC_8 in thf. To prevent the formation of the unwanted dianionic dimers $[M_2(CO)_{10}]^{2-}$,

(10) Fischer, R. A.; Miehr, A. *Chem. Mater.* **1996**, *8*, 497−508.
(11) Fischer, R. A.; Miehr, A.; Schulte, M. M. *Adv. Mater.* **1995**, *7*, 58−61.
(12) Fischer, R. A.; Miehr, A.; Herdtweck, E. *J. Chem. Soc., Chem. Commun.* **1995**, 337−338.
(13) Fischer, R. A.; Scherer, W.; Kleine, M. *Angew. Chem.* **1993**, *105*, 778−780; *Angew. Chem., Int. Ed. Engl.* **1993**, *32*, 748−750.
(14) Reed, A. E.; Curtiss, L. A.; Weinhold, F. *Chem. Rev.* **1988**, *88*, 899−926.
(15) Bader, R. F. W. *Atoms in Molecules. A Quantum Theory*; Oxford University Press: Oxford, 1990.
(16) Dapprich, S.; Frenking, G. *J. Phys. Chem.* **1995**, *99*, 9352−9362.
(17) Armer, B.; Schmidbaur, H. *Chem. Ber.* **1967**, *100*, 1521−1535.
(18) Gladysz, J. A.; Tam, W. *J. Org. Chem.* **1978**, *43*, 2279−2280.
(19) Schwindt, M. A.; Lejon, P.; Hegedus, L. S. *Organometallics* **1990**, *9*, 2814−2819.

Table 2. Selected Raman Data of M−Ga Complexes (Single Crystals)

compd no.	ν(CO)	ν(MGa)	ν(GaN)	ν(GaC)	ν(GaCl)	ν(MC)
6		166	490	526, 555		415, 428
8	2041 vs; 1960 m; 1901 m; 1890 vs	159	498		310	414, 417
9[a]	2031 vs; 1937 s, br; 1902 w					
9	2026 vs; 1925 vs; 1899 vs; 1888 m	161	499	575		415, 428
10	2039 vs; 1953 m; 1892 m; 1883 vs	156	499		313	441, 458
11[a]	2030 vs; 1932 vs; 1886 w					
11	2024 vs; 1919 vs; 1892 s; 1880 s	157	503	575		445, 449

[a] Data taken from CH_2Cl_2 solution between CaF_2 plates.

Table 3. ^{1}H NMR Data of Compounds **1**−**24**

compound	no.	CH_2CH_3 (q, 2H)	CH_2CH_3 (t, 3H)	NCH_3 (s, 6H)	NCH_2 (m, 4H, AA′BB′)
$(CO)_5Cr-Al[(Cl)(tmeda)]$	**15**			2.86, 2.92	3.24
$(CO)_5Cr-Al[(CH_2CH_3)(tmeda)]$	**16**	0.18 $^3J_{HH} = 8$ Hz	1.21 $^3J_{HH} = 8$ Hz	2.69, 2.92	2.96, 3.07
$(CO)_5Mo-Al[(Cl)(tmeda)]$	**17**			2.83, 2.90	3.18
$(CO)_5Mo-Al[(CH_2CH_3)(tmeda)]$	**18**	0.15 $^3J_{HH} = 7.9$ Hz	1.15 $^3J_{HH} = 7.9$ Hz	2.63, 2.84	3.00
$(CO)_5W-Al[(Cl)(tmeda)]$	**19**			2.79, 2.84	2.94, 3.18
$(CO)_5W-Al[(CH_2CH_3)(tmeda)]$	**20**	0.15 $^3J_{HH} = 7.9$ Hz	1.16 $^3J_{HH} = 7.9$ Hz	2.64, 2.86	2.98
$(CO)_5Cr-Ga[(Cl)(tmeda)]$	**2**			2.75, 2.80	3.11
$(CO)_5Cr-Ga[(CH_2CH_3)(tmeda)]$	**7**	0.57 $^3J_{HH} = 7.8$ Hz	1.24 $^3J_{HH} = 7.8$ Hz	2.55, 2.79	2.86
$(CO)_5Mo-Ga[(Cl)(tmeda)]$	**8**			2.65, 2.71	2.80, 3.07
$(CO)_5Mo-Ga[(CH_2CH_3)(tmeda)]$	**9**	0.47 $^3J_{HH} = 7.8$ Hz	1.18 $^3J_{HH} = 7.8$ Hz	2.50, 2.70	2.83
$(CO)_5W-Ga[(Cl)(tmeda)]$	**10**			2.65, 2.70	2.83, 3.06
$(CO)_5W-Ga[(CH_2CH_3)(tmeda)]$	**11**	0.49 $^3J_{HH} = 7.8$ Hz	1.15 $^3J_{HH} = 7.8$ Hz	2.51, 2.71	2.84
$(CO)_4Fe-Ga[(Cl)(tmeda)]$	**12**			2.82, 2.84	3.00, 3.10
$(CO)_4Fe-Ga[(CH_3)(tmeda)]$	**13**	0.09 (CH_3, s, 3H)		2.62, 2.81	2.98
$(CO)_4Fe-Ga[(CH_2CH_3)(tmeda)]$	**14**	0.73	1.24	2.63, 2.81	2.95
$(CO)_5Cr-Ga[(Cl)(dme)]$	**3**			2.09	4.18
$(CO)_5Cr-Ga[(Cl)(bipy)]$	**4**			7.90−7.94 (*m*), 8.34−8.41 (*o*), 8.90−8.92 (*p*)	
$(CO)_5Cr-Ga[(Cl)(^tBu\text{-}dab)]$	**5**			1.62 (s, 18H)	8.2 (s, 2H)
$(CO)_5Cr-Ga[(Me)(tmeda)]$	**6**	−0.01 (CH_3, s, 3H)		2.52, 2.79	2.87
$(CO)_5Cr-Ga[(H)(tmeda)]$	**21**	5.03 (GaH, s, 1H)		2.78, 2.83	3.14
$(CO)_5Cr-Ga[(BH_4)(tmeda)]$	**22**	1.50 (BH_4, q, br, 4H) $^1J_{BH} = 93$ Hz		2.68, 2.79	2.94, 3.00
$(CO)_5W-Al[(Cl)(tmpda)]$	**23**			2.69, 2.72	2.63, 3.52 1.82, 2.19 ($CH_2CH_2CH_2$)
$(CO)_5W-Al[(^iBu)(tmpda)]$	**24**	0.17 (CH_2, d, 2H, 6.8 Hz) 1.05 (CH_3, d, 6H, 6.45 Hz) 2.11 (CH, m, 1H, 6.6 Hz)		2.61, 2.74	2.45, 2.97 1.89, 2.19 ($CH_2CH_2CH_2$)

the reaction mixture should not be too concentrated (<1 mmol·mL^{-1}) and the reaction time must be longer than 4.5 h. A typical improved procedure is as follows: A suspension of 4.2 mmol of KC_8 in 60 mL of thf is cooled to −78 °C, and 2 mmol of the solid hexacarbonyl is added. The mixture is allowed to warm to room temperature and is stirred for a minimum of 5 h. In the case of molybdenum the color of the mixture turns to muddy beige or brown; for tungsten a gray-green color is observed. The mixtures prepared in this manner are used for further preparations. The IR spectra of the reaction solution exhibit no evidence for formation of the $[M_2(CO)_{10}]^{2-}$ species.

General Procedure for the Preparation of $(CO)_5M-E[X(L)_2]$ (M = Cr, Mo, W; E = Al, Ga; X = Cl, Me, Et, ^{i}Bu) (2−11, 15−20, 23, 24). According to the procedure above, a suspension of the dianion $[M(CO)_5]^{2-}$ (M = Cr, Mo, W) in thf is prepared in situ and cooled to −78 °C. Then a solution of a stoichiometric quantity (typically 2 mmol) of the respective aluminum or gallium compound in 20 mL of thf, also cooled to −78 °C, is added. The mixture is allowed to warm to room temperature and is stirred for 1 h. Then the desired bidentate Lewis base ligand (2 mmol) is added. After 30 min of stirring at 25 °C, the solvent is removed in vacuo and the residue is extracted with 50 mL of CH_2Cl_2. After the sedimentation of the graphite the yellow or orange solutions are slowly filtered using the cannula technique. In the case of the compounds **4** and **5** with Lewis bases exhibiting conjugated π-systems the solutions are colored deep blue and red, respectively. The obtained clear solutions are concentrated to a volume of 10 mL and are stored at −30 °C. From these solutions the compounds separate as well-shaped yellow to orange crystals. After the mother liquor is decanted and further concentration of a second crop the total yield rises typically to 92−98%. The crystals can be handled in air and are stable against moisture for a short time (several minutes). The compounds **3**−**5** crystallize not as well as the tmeda species do and are obtained as microcrystalline powders. The crystals of **15** seem to contain CH_2Cl_2 and decompose into a microcrystalline powder upon separation from the mother liquor.

For the alkyl complexes $(CO)_5M-Ga[R(L)_2]$ (M = Cr, Mo, W; R = Me, Et) a somewhat different synthesis is possible. The procedure is similar to that described above; however, twice the stoichiometric amount of dialkylgallium chloride R_2GaCl (R = Me, Et) is used per mole of the transition metal component. In this case, GaR_3 is formed as a byproduct and is evaporated with the solvent thf during the workup of the reaction mixture.

Synthesis of $(CO)_5Cr-Ga[Cl(thf)_2]$ (1) as a Solution in Dichloromethane. The compound $K_2[Cr(CO)_5]$ is synthesized in situ as descibed above. Then a stoichiometric quantity of $GaCl_3$ (typically 2 mmol) is added, and the reaction is conducted similarly to the procedure outlined above. The thf reaction mixture is filtered from the graphite,

Table 4. $^{13}C\{^1H\}$ NMR Data of the Compounds **1**−**24**

compound	no.	$\underline{C}H_2CH_3$	$CH_2\underline{C}H_3$	$(N\underline{C}H_3)$	$(\underline{C}H_2N)$	CO
$(CO)_5Cr-Al[(Cl)(tmeda)]$	**15**			48.3, 49.6	57.5	224.3, 229.0.
$(CO)_5Cr-Al[(CH_2CH_3)(tmeda)]$	**16**	9.0	27.7	48.5, 49.0	57.9	221.4, 231.9
$(CO)_5Mo-Al[(Cl)(tmeda)]$	**17**			46.7, 48.4	56.8	209.4, 214.6
$(CO)_5Mo-Al[(CH_2CH_3)(tmeda)]$	**18**	8.6	25.3	48.1, 48.7	57.2	210.2, 213.8
$(CO)_5W-Al[(Cl)(tmeda)]$	**19**			48.9, 49.5	57.2	206.0, 209.3
$(CO)_5W-Al[(CH_2CH_3)(tmeda)]$	**20**	9.1	26.2	49.0, 49.8	57.7	207.5, 211.2
$(CO)_5Cr-Ga[(Cl)(tmeda)]$	**2**			47.6, 48.2	57.0	223.4, 228.6
$(CO)_5Cr-Ga[(CH_2CH_3)(tmeda)]$	**7**	9.1	18.1	47.6, 49.1	58.0	228.2
$(CO)_5Mo-Ga[(Cl)(tmeda)]$	**8**			47.8, 48.3	57.3	211.8, 215.0
$(CO)_5Mo-Ga[(CH_2CH_3)(tmeda)]$	**9**	8.9	19.2	46.9, 50.0	57.8	216.6, 218.4
$(CO)_5W-Ga[(Cl)(tmeda)]$	**10**			47.9, 48.6	57.2	201.7, 204.2
$(CO)_5W-Ga[(CH_2CH_3)(tmeda)]$	**11**	9.2	19.5	47.0, 50.4	57.7	206.4, 208.0
$(CO)_4Fe-Ga[(Cl)(tmeda)]$	**12**			48.2, 49.2	57.2	217.4
$(CO)_4Fe-Ga[(CH_3)(tmeda)]$	**13**	1.4 q, $^1J_{CH} = 61$		48.4, 48.5 q, $^1J_{CH} = 139$ q, $^1J_{CH} = 139$	57.4 t, $^1J_{CH} = 139$	219.4
$(CO)_4Fe-Ga[(CH_2CH_3)(tmeda)]$	**14**	10.0 q, $^1J_{CH} = 126$	13.1 t, $^1J_{CH} = 119.6$	48.1, 48.6 q, $^1J_{CH} = 137$ q, $^1J_{CH} = 136$	57.5 t, $^1J_{CH} = 139$	219.4
$(CO)_5Cr-Ga[(Cl)(dme)]$	**3**			25.6	70.9	221.6, 227.2
$(CO)_5Cr-Ga[(Cl)(bipy)]$	**4**	122.8 (*m*-CH), 128.3 (*p*), 140.5 (*m*), 142.7 (*o*), 147.6 (*o*-CH)				223.4
$(CO)_5Cr-Ga[(Cl)(tBu-dab)]$	**5**	30.8 (CCH_3), 65.7 (CCH_3), 156.0 (N═CH)				212.4, 230.5
$(CO)_5Cr-Ga[(Me)(tmeda)]$	**6**	6.3 q, $^1J_{CH} = 120$		47.7, 48.9 q, $^1J_{CH} = 130$ q, $^1J_{CH} = 139$	57.8 t, $^1J_{CH} = 139$	227.9, 231.6
$(CO)_5Cr-Ga[(H)(tmeda)]$	**21**			47.2, 47.9	56.3	224.6
$(CO)_5Cr-Ga[(BH_4)(tmeda)]$	**22**			47.8, 47.9	59.0	226.9
$(CO)_5W-Al[(Cl)(tmpda)]$	**23**	21.5 ($CH_2\underline{C}H_2CH_2$)		46.2, 49.2	58.8	206.3
$(CO)_5W-Al[(^tBu)(tmpda)]$	**24**	21.8 ($CH_2\underline{C}H_2CH_2$) 26.7 ($\underline{C}H$) 28.5 ($\underline{C}H_3$) $Al-\underline{C}H_2$ not detected		48.4, 49.3	60.15	207.0

Table 5. Experimental Data of the Structure Determinations of Compounds **2**, **20**, and **23**

	2	**20**	**23**
formula	$C_{11}H_{16}ClCrGaN_2O_5$	$C_{13}H_{21}AlN_2O_5W$	$C_{12}H_{18}AlClN_2O_5W$
fw	413.43	496.15	516.56
crystal system	monoclinic	monoclinic	orthorhombic
space group	$P2_1/n$ (no. 14)	$P2_1/n$ (no. 14)	*Pccn* (no. 56)
λ, Å	0.71073	0.71073	0.71073
a, Å	9.059(4)	8.606(2)	23.990(6)
b, Å	16.084(7)	16.463(6)	9.044(3)
c, Å	11.835(6)	12.469(4)	15.871(4)
β, deg	80.61(3)	93.88(2)	90.0
V, Å^3	1701.3(14)	1762.6(9)	3443.5(17)
Z	4	4	8
ρ_{calc}, g cm^{-3}	1.614	1.870	1.993
μ (Mo Kα), cm^{-1}	2.397	6.625	6.937
no. of reflns	3169	4065	3777
no. of obsd reflns	2496	3280	2457
cutoff	$I > 2.0\sigma(I)$	$I > 2.0\sigma(I)$	$I > 2.0\sigma(I)$
R^a	0.037	0.027	0.044
$R_w{}^b$	0.111	0.065	0.088

[a] $R = \sum(||F_o| - |F_c||)/\sum|F_o|$. $R_w = [\sum w(F_o^2 - F_c^2)^2/\sum w(F_o^2)^2]^{1/2}$.

and the solvent is removed in vacuo. The residue is extracted twice with a mixture of CH_2Cl_2/thf (10:1 volume parts). This is necessary to achieve quantitative separation from the byproduct KCl, which has a significant solubility in thf. The red-colored extracts are combined, the solvent is evaporated in vacuo, and the off-white, slightly red (from an unknown trace impurity) residue is dried extensively in vacuo at 25 °C. The empirical formula of $C_5ClCrGaO_5$ for this solid residue is obtained from a total elemental analysis. This product (**1a**) is insoluble in CH_2Cl_2 and other noncoordinating (toluene) or weakly coordinating (diethyl ether) solvents. It completely dissolves into CH_2Cl_2 by adding exactly 2 equiv of thf. All the other Lewis base adducts can be obtained from **1a** by adding the respective base ligand to the suspension of **1a** in CH_2Cl_2.

Synthesis of Hydrido(pentacarbonylchromio)(tetramethylethylenediamino)gallium (21). A sample of 827 mg (2 mmol) of $(CO)_5Cr-Ga[(Cl)(tmeda)]$ (**2**) is dissolved in 40 mL of thf and cooled to −78 °C. A portion of 318 mg (40 mmol) of LiH is added, and the reaction mixture is allowed to warm to room temperature. After 12 h with vigorous stirring the color of the solution is red. After filtration and evaporation of the solvent the residue is extracted with toluene. The toluene is evaporated in vacuo. Compound **21** (580 mg, 76%) is obtained as an off-white microcrystalline powder. Selected spectroscopic data: ^1H NMR (270.16 MHz, CD_2Cl_2, 25 °C) δ 5.03 (s, br 1 H, GaH); ^-IR (CH_2Cl_2, cm^{-1}) ν(GaH) = 1835 (m, br).

Synthesis of (Tetrahydridoboranato)(pentacarbonylchromio)(tetramethylethylenediamino)gallium (22). A sample of 414 mg (1 mmol) of $(CO)_5Cr-Ga[(Cl)(tmeda)]$ (**2**) is dissolved in 40 mL of thf and cooled to −78 °C. To that solution is added a quantity of 2 g (50 mmol) of $NaBH_4$, and the reaction mixture is allowed to warm to room temperature. After being vigorously stirred for 12 h the reaction mixture

is worked up as decribed for compound **21** above. Selected spectroscopic data: ^{1}H NMR (399.78 MHz, CD_2Cl_2, 25 °C) $\delta = 1.50$ (q, br, 4 H, BH_4, $^1J_{BH} = 93$ Hz); ^{11}B{^{1}H} NMR (128.27 MHz, CD_2Cl_2, 25 °C) $\delta = -10.8$; IR (Toluol, cm^{-1}) ν(BH) = 2380 (w, br), 2324 (vw), 2278 (w).

Single-Crystal X-ray Diffraction Analysis of 2, 20, and 23. Crystals of compounds **2**, **20**, and **23** were grown by standard cooling techniques at low temperature from CH_2Cl_2 solutions (see above). Preliminary examination and data collection were carried out on a Siemens Nicolet Syntex R3m/V diffractometer. Final cell constants were obtained by least-squares refinements of 25 automatically centered high-angle reflections. During data collection, the orientation and intensity of three control reflections were monitored after every 50th reflection. Crystal data and intensity collection parameters together with details of the refinement are summarized in Table 5. In a similar way single-crystal structure data have also been obtained for compounds **6**, **7**, **11**, and **12**.[6,20] These latter results will be published elsewhere. Further information can be obtained from the Supporting Information or directly from the authors (R.A.F and L.Z).

Computational and Theoretical Methods

The geometry optimizations have been carried out at the MP2 level of theory[21,22] using our standard basis set II,[29] which has a relativistic effective core potential (ECP) and a (441/2111/21) split-valence basis set for tungsten,[23] a 6-31G(d) all electron basis set for H, C, N, O, and Al,[24−26] and a pseudopotential with a (31/31/1) valence basis set for Cl, Ga, In, and Tl.[27,28] The calculations have been carried out using the program packages Gaussian 94[30a] and Turbomole.[30b]

To see if the calculated structures are minima on the potential energy surface, we first optimized the geometries of $(CO)_5WAl[H(NH_3)_2]$, $(CO)_5WAl[Cl(NH_3)_2]$, $(CO)_5WAlH$, $(CO)_5WAlCl$, $Al[H(NH_3)_2]$, and $Al[Cl(NH_3)_2]$ at the HF/II level of theory followed by numerical calculations of the Hessian matrix. The optimized geometries were found to be true minima (only positive eigenvalues of the Hessian) at HF/II. The HF/II optimized structures were taken as starting geometries for the MP2/II optimization. We did not calculate vibrational frequencies at MP2/II, and we did not calculate vibrational frequencies for **M3**−**M6**. We believe, however, that the MP2/II optimized structures are energy minima.

The bonding situation of the compounds was analyzed using the natural bond orbital (NBO) method developed by Weinhold[14] and the topological analysis of the electron density distribution developed by Bader.[15] The metal−ligand donor−acceptor interaction was investigated with the newly developed charge-decomposition analysis (CDA).[16] In the CDA method the (canonical or natural) molecular orbitals of the complex are expressed in terms of the MOs of appropriately chosen fragments. In the present case, the natural orbitals (NO) of the MP2/II wave function of $(CO)_5W-L$ have been formed by a linear combination of the MOs of $(CO)_5W$ and L in the geometry of $(CO)_5WL$. The orbital contributions to the electronic charge are then divided into three parts: (i) L → $W(CO)_5$ donation d given by the mixing of the occupied MOs of L and the unoccupied MOs of $W(CO)_5$; (ii) $(CO)_5W$ → L back-donation b given by the mixing of the unoccupied MOs of L and the occupied MOs of $W(CO)_5$; and (iii) $(CO)_5W$ ↔ L repulsive polarization r given by the mixing of the occupied MOs of L and $W(CO)_5$. The analyses of the Al−N interactions are carried out in a similar way by choosing $2NH_3$ as one fragment, and $(CO)_5WAlX$ or AlX (X being hydrogen or chlorine) as the other fragment. A more detailed presentation of the method and the interpretation of the results is given in refs 16 and 73. The CDA calculations have been performed using the program CDA 2.1.[31]

Results and Discussion

A. Synthesis and Properties. In contrast to the well-developed chemistry of (organo) group-13 halides $X_{3-a}ER_a$ (*X* = halide; R = alkyl, aryl) with carbonylmetal monoanions only very few reports on the related reactivity toward dianions exist. Noteworthy are some reports on indium and thallium transition metal compounds with special bonding situations, e.g., metallacumulenes and M−In(I) donor−acceptor interactions.[32−35] For the lighter homologues, e.g., gallium, we recently communicated the dianionic "iniden" complexes $\{[(CO)_nM]_2(\mu\text{-GaR}\}^{2-}$ (M = Fe, *n* = 4, R = Me; M = Cr, *n* = 5, R = Me, Et), the monoanionic complexes $\{(CO)_nM-Ga(X^1X^2(L)\}^-$ (M = Cr, Fe; *n* = 4, 5; $X^1 = X^2 = Cl$; $X^1 = Cl$, X^2 = Me, Et) and $\{(CO)_nM-Ga[(CH_2)_3NMe_2](X)\}^-$ (M = Cr, Mn, Fe; L = NO, CO; *n* = 3, 4; X = Cl, Me, ^{t}Bu)[36] as well as the neutral complexes $(CO)_4Fe\{Ga[(CH_2)_3NMe_2](R)\}_2$ (R = ^{t}Bu, Ph) and $\{(CO)_4Fe-Ga[(CH_2)_3NMe_2]\}_2$.[37] Some iron compounds of the type $(CO)_4Fe-[Ga(R)L_2]$ had previously been claimed on the basis of IR and NMR data, but no structural information was given.[38]

Gallium Chemistry. The reaction between equimolar quantities of $GaCl_3$ or alkylgallium dichlorides with carbonylmetalate dianions in thf initially leads to the monoanionic intermediates $\{(CO)_nM-Ga[X(Cl)]\}^-$ (M = Fe, Cr; *n* = 4, 5; X = Cl, Me, Et) which can be isolated as solvent free salts after cation exchange with a noncoordinating counterion, e.g., PPN^+ Ph_4P^+, or Ph_4As^+ (Scheme 1).[36] The compound $[(CO)_5Cr-GaCl_2]$-[K(thf)] was isolated from the reaction solution without cation exchange (total elemental analysis). This species eliminates a second equivalent KCl upon treatment of the solid with CH_2Cl_2 to form the neutral bis-thf complex $(CO)_5Cr-Ga[(Cl)(thf)_2]$ (**1**) and an insoluble transition metal complex **1a** besides KCl. The insoluble species can be converted into **1** upon addition of exactly 2 equiv of thf (Scheme 1). Compound **1** could not be isolated in pure form because of the facile loss of thf. The empirical formula of the solid **1a** remaining after drying in vacuo

(20) Schulte, M. M. Ph.D. Thesis, TU München, **1996**.
(21) Möller, C.; Plesset, M. S. *Phys. Rev.* **1934**, *46*, 618−632.
(22) Binkley, J. S.; Pople, J. A. *Int. J. Quantum Chem.* **1975**, *9*, 229−236.
(23) Hay, P. J.; Wadt, W. R. *J. Chem. Phys.* **1985**, *82*, 299−310.
(24) Hehre, W. J.; Ditchfield, R.; Pople, J. A. *J. Chem. Phys.* **1972**, *56*, 2257−2261.
(25) Hariharan, P. C.; Pople, J. A. *Theor. Chim. Acta* **1973**, *28*, 213−222.
(26) Gordon, M. S. *Chem. Phys. Lett* **1980**, *76*, 163−168.
(27) Bergner, A.; Dolg, M.; Küchle, W.; Stoll, H.; Preuss, H. *Mol. Phys.* **1993**, *80*, 1431−1441.
(28) The exponents of the d-type polarization functions are 0.650 (Cl), 0.207 (Ga), 0.160 (In), and 0.150 (Tl). They have been taken from Andzelm, J.; Huzinaga, S.; Klobukowski, M.; Radzio, E.; Sakai, Y.; Tatekawi, H. *Gaussian Basis Sets for Molecular Calculations*; Elsevier: Amsterdam, 1984.
(29) Frenking, G.; Antes, I.; Böhme, M.; Dapprich, S.; Ehlers, A. W.; Jonas, V.; Neuhaus, A.; Otto, M.; Stegmann, R.; Veldkamp, A.; Vyboishchikov, S. F. In *Reviews in Computational Chemistry*; Lipkowitz, K. B., Boyd, D. B., Eds.; VCH: New York, 1996; Vol. 8, p 63.
(30) (a) Gaussian 94: Frisch, M. J.; Trucks, G. W.; Schlegel, H. B.; Gill, P. M. W.; Johnson, B. G.; Robb, M. A.; Cheeseman, J. R.; Keith, T. A.; Petersson, G. A.; Montgomery, J. A.; Raghavachari, K.; Al-Laham, M. A.; Zakrzewski, V. G.; Ortiz, J. V.; Foresman, J. B.; Cioslowski, J.; Stefanov, B. B.; Nanayakkara, A.; Challacombe, M.; Peng, C. Y.; Ayala, P. Y.; Chen, W.; Wong, M. W.; Andres, J. L.; Replogle, E. S.; Gomberts, R.; Martin, R. L.; Fox, D. J.; Binkley, J. S.; Defrees, D. J.; Baker, I.; Stewart, J. J. P.; Head-Gordon, M.; Gonzalez, C.; Pople, J. A., Gaussian Inc., Pittsburgh, PA, 1995. (b) Häser, M.; Ahlrichs, R. J. *J. Comput. Chem.* **1989**, *10*, 104−111.
(31) CDA 2.1: Dapprich, S.; Frenking, G., Marburg, 1994.
(32) Reger, D. L.; Mason, S. S.; Rheingold, A. L.; Haggerty, B. S.; Arnold, F. P. *Organometallics* **1994**, *13*, 5049−5053.
(33) Atwood, J. L.; Bott, S. G.; Hitchcock, P. B.; Eaborn, C. B.; Shariffudin, R. S.; Smith, J. D.; Sullivan, A. C. *J. Chem. Soc., Dalton Trans.* **1987**, 747−755.
(34) Huttner, G.; Schiemenz, B. *Angew. Chem.* **1993**, *105*, 1840−1841; *Angew. Chem., Int. Ed. Engl.* **1993**, *32*, 1772−1773.
(35) Curnow, O. J.; Schiemenz, B.; Huttner, G.; Zsolnai, L. *J. Organomet. Chem.* **1993**, *459*, 17−20.
(36) Schulte, M. M.; Fischer, R. A.; Herdtweck, E.; Mattner, M. R. *Inorg. Chem.* in press.
(37) Fischer, R. A.; Schulte, M. M.; Priermeier, T. *J. Organomet. Chem.* **1995**, *493*, 139−142.
(38) Cymbaluk, T. H.; Ernst, R. D. *Inorg. Chem.* **1980**, *19*, 2381−2384.

Scheme 1. Synthesis of Compounds **1**−**24** (E = Al, Ga; n = 5 for M = Cr, Mo, and W; n = 4 for M = Fe; L_2 = ^{t}Bu-dab, bipy, $Me_2N(CH_2)_mNMe_2$ (m = 2 for tmeda; m = 3 for tmpda); X = Cl, alkyl; R = alkyl, H, BH_4)

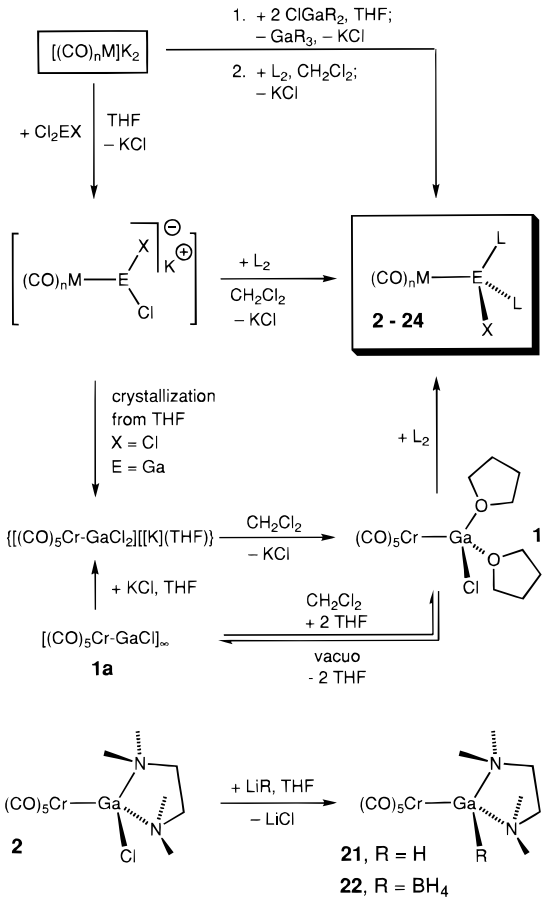

is $C_5ClCrGaO_5$. This agrees with a species of the type $[(CO)_5Cr-GaCl]$ which is likely to have an associated structure similar to the known coordination polymer compound $[(CO)_5Cr-In(Br)(thf)]$ where the indium center is pentacoordinated via bridging bromide ligands.[39] The NMR and IR data of **1** are very similar to those of $[(CO)_5Cr-Ga(Cl)(dme)]$ (**3**). Complex **1** can be viewed as the key compound to the new class of complexes described herein. On addition of a chelating (hard) Lewis base like tmeda, or dme, the stable chromium gallium complexes **2**−**5** are obtained. The corresponding alkylated complexes **6** and **7** and the related molybdenum, tungsten, and iron compounds **8**−**14** are obtained similarly (Scheme 1).

If equimolar quantities of carbonylmetalate dianions and dialkylgallium chlorides are combined, the primary formed monoanionic intermediates $[(CO)_nM-GaR_2]^-$ (M = Fe, Cr; R = Me, Et) are unstable. Rapid ligand redistribution occurs and GaR_3 is split off to yield the stable dianionic "iniden" complexes $\{(\mu\text{-GaR})[(CO)_nM]_2\}^{2-}$.[36] An alternative route to compounds such as **6** or **7** is based on this chemistry when twice the stoichiometric amount of R_2GaCl with respect to the carbonylmetalate is used (Scheme 1).

The metal complexes were obtained from concentrated CH_2Cl_2 solutions at −30 °C as large yellow to orange or yellow-green crystals. With soft Lewis base ligands, e.g., chelating phosphines (dmpe, dppe), or ligands exhibiting significant acceptor capabilities such as bipy or ^{t}Bu-dab, similar complexes were formed as intermediate species. However, it was very difficult to isolate and purify these compounds in acceptable yields. In the crystalline state the new compounds are surprisingly stable against air and for a short time against moisture. This is in remarkable contrast to the related complexes $(CO)_5M'-Al[(X)_2L]$ (M′ = Mn, Re) which decompose instantaneously when exposed to air.

Aluminum Chemistry. Nothing was known about the related chemistry of aluminum halides with carbonylmetalate dianions prior to our work. The neutral aluminum complexes $(CO)_5M-Al[(X)L_2]$ (X = Cl, Et, ^{i}Bu) (**15**−**20**, **23**, **24**) (Scheme 1) are accessible by the same procedure as discussed above. These complexes add to the rare number of compounds with nonbridged terminal M−Al bonds at transition metal carbonyl fragments.[8,40] Usually the formation of isocarbonyl M−CO−Al structures is preferred.[41−46] Structurally characterized examples for transition metal aluminum complexes *without* CO ligands are $[(\eta^5\text{-}C_5H_5)_2Ti-AlEt_2]_2$,[47] $[(\eta^5\text{-}C_5H_5)Ni-Al(\eta^5\text{-}C_5Me_5)]_2$,[48] $\{[(\eta^5\text{-}C_5Me_5)(\eta^2\text{-}C_2H_4)]Co-AlEt_2\}_2$,[49] or species such as $[(\eta^5\text{-}C_5H_5)(PMe_3)_2]Rh-Al_2Me_4Cl_2$.[50] In the case of a suitable combination of very nucleophilic transition metal carbonylates with steric and electronic shielding of the aluminum center an unbridged M−Al bond is preferred over the isocarbonyl bridging mode, e.g., $[(\eta^5\text{-}C_5H_5)(CO)_2]Fe-Al[(CH_2)_3NMe_2](^{i}Bu) and related compounds.[8] Following this strategy the related transition metal lanthanide complexes $[(\eta^5\text{-}C_5H_5)(CO)_2]Ru-Lu[(\eta^5\text{-}C_5H_5)_2(thf)]$ were recently reported.[51]

Ligand Exchange Experiments. A stream of CO (1 atm) was bubbled trough a thf solution of $(CO)_5W-Al[(X)(tmpda)]$ (X = Cl, alkyl) at ambient temperature for several hours. The *quantitative* formation of $(CO)_6W$ and the separation of an insoluble aluminum-containing but tungsten free, however not yet identified, byproduct was observed (elemental analysis). A related cleavage of the M−E bond takes place as a more or less important side reaction during the typical synthetic procedure of the compounds, however depending greatly on the conditions. Prolonged reaction times and higher temperatures, as well as the use of chelating Lewis base ligands with acceptor properties (bipy, ^{t}Bu-dab), give rise to the formation of $(CO)_4WL_2$. For example, treatment of $(CO)_5W-Al[(X)(tmpda)]$ with excess ^{t}Bu-dab for 12 h in thf solution under reflux gave $(CO)_4W($^{t}Bu-dab) besides $(CO)_6W$. The fate of the aluminum fragment in these cases is rather interesting and clearly warrants further investigations.

B. Spectroscopic Characterization. NMR Spectra. The ^{1}H NMR spectra of the complexes **2**, and **6**−**22** with the tmeda

(39) Behrens, H.; Moll, M.; Sixtus, E.; Thiele, G. *Z. Naturforsch.* **1977**, *32b*, 1109−1113.
(40) Burlitch, J. M.; Leonowicz, M. E.; Petersen, R. B.; Hughes, R. E. *Inorg. Chem.* **1978**, *18*, 1097−1105.
(41) Butts, S. B.; Holt, E. M.; Strauss, S. H.; Alcock, N. W.; Stimson, R. E.; Shriver, D. F. *J. Am. Chem. Soc.* **1979**, *101*, 5864−5866.
(42) Grimmett, D. L.; Labinger, J. A.; Bonfiglio, J. N.; Masuo, S. T.; Shearin, E.; Miller, J. S. *Organometallics* **1983**, *2*, 1325−1332.
(43) Petersen, R. B.; Stezowski, J. J.; Wan, C.; Burlitch, J. M.; Hughes, R. E. *J. Am. Chem. Soc.* **1971**, *93*, 3532−3534.
(44) Lukehart, C. M.; Torrence, G. P.; Zeile, J. V. *J. Am. Chem. Soc.* **1975**, *97*, 6903−6904.
(45) Kim, N. E.; Nelson, N. J.; Shriver, D. F. *Inorg. Chim. Acta* **1973**, *7*, 393−396.
(46) Conway, A. J.; Gainsford, G. J.; Schrieke, R. R.; Smith, J. D. *J. Chem. Soc., Dalton Trans.* **1975**, 2499−2506.
(47) Corradini, P.; Sirigu, A. *Inorg. Chem.* **1967**, *6*, 601−605.
(48) Dohmeier, C.; Krautscheid, H.; Schnöckel, H. *Angew. Chem.* **1994**, *106*, 2570−2572; *Angew. Chem., Int. Ed. Engl.* **1994**, *33*, 2482−2484.
(49) Schneider, J. J.; Krüger, C.; Nolte, M.; Abraham, I.; Ertel, T. S.; Bertagnolli, H. *Angew. Chem.* **1994**, *106*, 2537−2538; *Angew. Chem., Int. Ed. Engl.* **1994**, *33*, 2435−2436.
(50) Mayer, J. M.; Calabrese, J. C. *Organometallics* **1984**, *3*, 1292−1298.
(51) Beletskaya, I. P.; Voskoboynikov, A. Z.; Chuklanova, E. B.; Kirillova, N. I.; Shestakova, A. K.; Parshina, I. N.; Gusev, A. I.; Magomedov, G. K.-I. *J. Am. Chem. Soc.* **1993**, *115*, 3156−3166.

ligand exhibit diastereotopic *N*-methyl protons and typically reveal two signals. Depending on the degree of conformational flexibility of the chelate ring at the group-13, metal center more or less complex coupling patterns for the methylene units are observed expectedly. The ^{13}C NMR spectra are as expected without unusual features. The ^{27}Al NMR data for the halide complexes **15**−**20** show a broad resonance (typical line widths of 4600−5200 Hz) within the range from 156 to 176 ppm (with a AlCl moiety). The alkyl species **16**, **18**, and **20** resonate around 220 ppm at the low-field end for tetracoordinated aluminum compounds.[20] Typical tetracoordinated dialkyl Al(R)$_2$L transition metal aluminum compounds exhibit resonance within 180−215 ppm, whereas halide-substituted systems such as [(η^5-C_5H_5)(CO)$_2$]Fe−Al[Cl$_2$(thf)] resonate at 156 ppm.[8] Contrasting this, the ^{27}Al NMR shift of the complex [(η^5-C_5Me$_5$)Al−Fe(CO)$_4$] is close to 0 ppm, which is a consequence of the higher coordination number of 6.[5]

Mass Spectra. The fragmentation of the new (CO)$_n$M−Al[X(L)$_2$] complexes differs significantly from their (CO)$_n$M−Al[(X)$_2$L] congeners. Species with intact M−E bonds are comparatively abundant under the conditions of chemical ionization with isobutene. The molecule ion peaks are observed in a relative intensity up to 30%. The splitting off of the tmeda and the CO ligands is clearly preferred. In contrast, the related systems [L(CO)$_n$]M−E[X^{1}X^2(L)] show a dominant M−E bond splitting due to the relatively high stability of the X$_2$E$^+$ cations.[52] For (CO)$_4$Fe−Ga[Cl(tmeda)] (**12**) [M]$^+$ is observed in 21% relative intensity. Further fragments with an intact Fe−Ga bond are [M$^+$ − CO] (4%), [M$^+$ − Cl] (6%), and [M$^+$ − Cl − CO − tmeda] (18%). For complex **6** the molecule ion peak is observed in 5% relative intensity while the most intensive Cr−Ga fragment is [(CO)$_5$Cr−Ga(Me)]$^+$ (20%) besides peaks for the decarbonylated species [(CO)$_4$Cr−Ga(Me)]$^+$ and [(CO)$_3$Cr−Ga(Me)]$^+$. Complex **9** shows the loss of ethylene via a β-H elimination, and the fragment (CO)$_5$Mo−Ga[H(tmeda)]$^+$ is detected (19%).

Vibrational (ν(CO)) Spectra. The IR absorptions in the ν(CO) range between 1880 and 2030 cm^{-1} of the neutral product complexes (Table 1) are shifted to significant higher energies than those of the anionic intermediates of 1830−2000 cm^{-1}.[36] For the dme complex **3** the ν(CO) absorptions are 2040, 1953, and 1913 cm^{-1} (CH_2Cl_2), being almost identical with the postulated bis-thf species **1**. In general, the ν(CO) absorptions for the chloro derivatives are shifted hypsochromic about 20 cm^{-1} compared to the corresponding alkyl compounds which agrees with the qualitative expectation that the overall donor capacity of the halide-substituted EX fragment toward the transition metal fragment should be *lower*. A comparison of the ν(CO) frequencies of some of the neutral iron−gallium products with those of the primary formed anionic intermediats is interesting. For the isolated anionic species {(CO)$_4$Fe−Ga[(Cl)(R)]}[PPN] the ν(CO) bands are observed at 1997, 1906, and 1877 cm^{-1} (R = Me) and 1996, 1907, and 1876 cm^{-1} (R = Et) which are shifted to somewhat higher wavenumbers than those of the neutral compounds (CO)$_4$Fe−Ga[R(tmeda)] (**12**, R = Me; **13**, R = Et; 1992, 1905, 1863 cm^{-1}). This is against the general trend that the ν(CO) absorptions of neutral or cationic carbonyl complexes are observed at *higher* wavenumbers than those of closely related anionic species. This effect may be explained by a localization of electron density at the chloro ligand. In other words, the chloride leaving group is already preformed in the anionic intermediates and easily splits off. The anionic intermediates may thus be viewed as weak Lewis base adducts of the base chloride to the respective neutral EX products. It has to be pointed out that the *base free* congener of this series of Fe−Ga compounds, the complex (CO)$_4$Fe−Ga(C_6H_3Mes*$_2$) (Mes* = 2,4,6-^{i}Pr$_3$C$_3$H$_2$),[5b] exhibts significantly higher wavenumbers of 2032, 1959, 1941, and 1929 cm^{-1}. This is apparently a consequence of the Fe−Ga multiple bond interaction in this latter case. In compounds of type **12**−**13** this (weak) d_π−p_π back-bonding is switched off by the coordination of the Lewis base at the Ga center (see also sections D and E).

The compounds do not undergo a solvent dependent heterolytic dissociation into solvated ion pairs of the type [(CO)$_n$M]$^{2-}$ and [E(X)L$_2$]$^{2+}$. The M−E bonds are stable even in solvents such as acetonitrile and HMPT. This contrasts the behavior of the systems (CO)$_n$M′−E[(X)$_2$L] which completely dissociate into [(CO)$_n$M′]$^-$ and E[(X)$_2$L]$^+$ in polar coordinating solvents.

The Raman ν(CO) spectra of compounds **9** and **11** in CH_2Cl_2 solution exhibit three absorptions in the ν(CO) region (Table 2). The energies fit well with those observed in the IR spectra (Table 2), and the intensities are inverse as expected (weak intensity for the E mode and strong for the A modes). Because for molecules with a local $C_{4\nu}$ symmetry four Raman-active ν(CO) absorptions ($2A_1 + B_1 + E$) are required, we suppose, regarding the relative intensities, that the A_1(a) and the B_1 modes overlap. Due to the reduced symmetry in the crystal,[53] the respective RAMAN spectra show four absorptions in the ν(CO) region. The strong infrared E absorption split into two weak Raman-active B bands.

The data of Tables 1 and 2 compare very well with those of reference compounds of the type (CO)$_5$M−L, where L acts as a strong 2e Lewis base donor (L = pyridine, PR$_3$),[54−59] and with the respective data of the isoelectronic donor-stabilized transition metal silylene complexes (CO)$_5$M-SiR$_2$L.[60−62]

The low-energy stretching frequencies of the M−Ga, Ga−N, Ga−C, Ga−Cl, and M−C bonds of compounds **6** and **8**−**11** were obtained from single-crystal Raman measurements as well (Table 2). The M−Ga (M = Cr, Mo, W) stretching frequencies range from 156 to 166 cm^{-1} and are relatively independent of the transition metal or the substitution pattern on the gallium center.

Mössbauer Spectroscopy. Compound **12** serves as a representative example. The ^{57}Fe Mössbauer spectrum of a powder sample at 50 K shows a quadrupolar splitting of 1.706 ± 0.004 mm s^{-1} which is typical for trigonal bipyramidal (CO)$_4$Fe−L complexes with L in an axial position.[63−65] The isomeric shift of −0.1103 ± 0.002 mm s^{-1} is virtually identical with the

(52) Kronseder, C.; Schindler, T.; Berg, C.; Fischer, R. A.; Niedner-Schatteburg, G.; Bondybey, V. E. *J. Organomet. Chem.* **1994**, *475*, 247−256.

(53) Nakamoto, K. *Infrared Spectra of Inorganic and Coordination Compounds*, 2nd ed.; Wiley Intersience: New York, 1970.

(54) Graham, W. A. G. *Inorg. Chem.* **1968**, *7*, 315−321.

(55) Davies, M. S.; Pierens, R. K.; Aroney, M. J. *J. Organomet. Chem.* **1993**, *458*, 141−146.

(56) Cotton, F. A.; Kraihanzel, C. S. *J. Am. Chem. Soc.* **1962**, *84*, 4432−4439.

(57) Kraihanzel, C. S.; Cotton, F. A. *Inorg. Chem.* **1963**, *2*, 533−540.

(58) Cotton, F. A. *Inorg. Chem.* **1964**, *3*, 702−711.

(59) Cotton, F. A.; Musco, A.; Yagupsky, G. *Inorg. Chem.* **1967**, *6*, 1357−1364.

(60) Chauhan, B. P. S.; Corriu, R. J. P.; Lanneau, G. F.; Priou, C.; Auner, N.; Handwerker, H.; Herdtweck, E. *Organometallics* **1995**, *14*, 1657−1666.

(61) Zybill, C.; Müller, G. *Angew. Chem.* **1987**, *99*, 683−684; *Angew. Chem., Int. Ed. Engl.* **1987**, *26*, 669−670.

(62) Zybill, C.; Müller, G. *Organometallics* **1988**, *7*, 1368−1372.

(63) Farmery, K.; Kilner, M.; Greatrex, R.; Greenwood, N. N. *J. Chem. Soc. (A)* **1969**, 2339−2345.

(64) Sosinsky, B. A.; Noren, N.; Shong, R. G. *Inorg. Chem.* **1982**, *21*, 4229−4233.

(65) Watanabe, M.; Sano, H. *Bull. Chem. Soc. Jpn.* **1990**, *63*, 777−784.

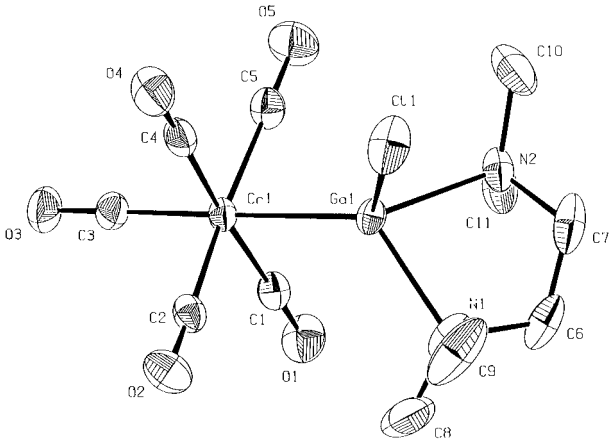

Figure 1. Molecular structure of $(CO)_5Cr-Ga[(Cl)(tmeda)]$ (**2**) in the crystal (ORTEP drawing; hydrogen atoms are omitted). Selected bond lengths (Å) and angles (deg): Ga−Cr 2.456(1), Ga−N(1) 2.163(4), Ga−N(2) 2.140(3), Ga−Cl 2.269(2), Cr−C(1) 1.902(4), Cr−C(2) 1.900(4), Cr−C(3) 1.865(4), Cr−C(4) 1.900(4), Cr−C(5) 1.905(4); Cr−Ga−N(1) 124.8(1), Cr−Ga−N(2) 124.6(1), Cr−Ga−Cl 120.8(1), N(1)−Ga−N(2) 83.6(2), N(1)−Ga−Cl 98.3(1), N(2)−Ga−Cl 95.8-(1), Ga−Cr−C(1) 88.8(1), Ga−Cr−C(2) 86.2(1), Ga−Cr−C(3) 178.2-(1), Ga−Cr−C(4) 87.1(1), Ga−Cr−C(5) 85.9(1).

value of −0.11 for the complex $(CO)_4Fe-P(NMe_2)_3$ but differs somewhat from the Fe^0 reference compound $Fe(CO)_5$ of −0.09.

Electronic Spectroscopy. Luminescence from transition metal stabilized AlX complexes $(CO)_5W-Al[(X)(tmpda)]$ (X = Cl, ^{i}Bu) (**23**, **24**) is observed in the visible spectral region. The lowest-energy electronic transition in these compounds is assigned as a d−d band on the basis of the long luminescence lifetime observed in low-temperature glasses and the weak absorption band. The characteristics of the electronic spectra are discussed elsewhere in detail. The similarity to reference compounds of the type $(CO)_5W-L$ (L = pyridine, etc.) was clearly established.[66]

C. Structures. The compounds **2**, **20**, and **23** are monomeric in the solid state without noticeably short intermolecular contacts (Figures 1−3). The Cr−Ga bonds of **2** (as well **6** and **7**[6,20]) and the W−Al bonds of **20** and **23** are unprecedented for molecular compounds. The metal−metal distances range around the sum of the covalent radii. The W−Al distance of 2.670(1) Å in compound **20** compares well with those of hydride-bridged W−Al bonds ranging from 2.62 to 2.69 Å.[68,69] One noticeable feature of the series of structures presented here and other related ones is the shortening of the M−E bond when alkyl substituents at the group-13 element are replaced by halide residues. A good example is the series $[(PPh_3)(CO)_3]Co-Ga\{[(CH_2)_3NEt_2]-(CH_3)\}$[7] with 2.496(1) Å, $[(PPh_3)(CO)_3]Co-Ga\{[(CH_2)_3NEt_2]-(Cl)\}$[7] with 2.372(1), and $[(Me_3P)(CO)_3]Co-GaCl_2(NMe_3)$ with 2.342(1) Å.[70,71] Also M−E bond distances are known to cover a broad range depending on the particular ligand surrounding the metal centers as shown by the comparison of $[(\eta^5\text{-}C_5Me_5)-Al-Fe(CO)_4]$ (2.231(3) Å) with $[(\eta^5\text{-}C_5H_5)(CO)_2]Fe-Al\{[(CH_2)_3-NMe_2](^iBu)\}$[8] (2.456(1) Å) and $(CO)_4Fe-Ga[(Cl)(tmeda)]$ (2.33.8(2) Å) with $[(\eta^5\text{-}C_5H_5)(CO)_2]Fe-Ga[Cl_2(NMe_3)]$ (2.3618-(3) Å)[7] and with $[(\eta^5\text{-}C_5H_5)(CO)_2]Fe-Ga\{[(CH_2)_3NMe_2](Et)\}$ (2.457(1) Å).[71] The shortest Fe−Ga bond to date of 2.248(7) Å was observed for $(CO)_4Fe-Ga(C_6H_3Mes^*_2)$ (Mes* = 2,4,6-^{i}Pr$_3$C$_3$H$_2$), which contains a linear dicoordinated Ga center, while all other cited Fe−Ga distances refer to tetracoordinated Ga centers.[5b] For **2** the Ga−Cl bond length of 2.269(2) Å appears somewhat long, compared with other Ga−Cl bonds (typically ranging around 2.16 ± 0.05 Å) in compounds with tetracoordinated gallium centers. A discussion of the metal group-13 element bonding with respect to the structural features of the compounds is given in the next section.

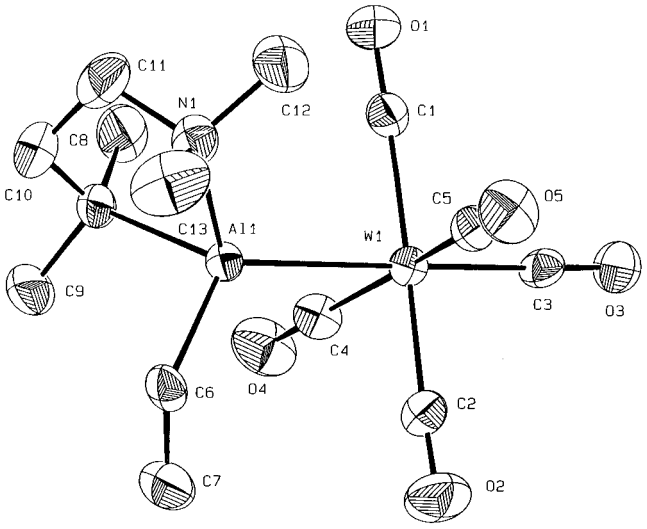

Figure 2. Molecular structure of $(CO)_5W-Al[(CH_2CH_3)(tmeda)]$ (**20**) in the crystal (ORTEP drawing; hydrogen atoms are omitted). Selected bond lengths (Å) and angles (deg): Al−W 2.670(1), Al−N(1) 2.095-(4), Al−N(2) 2.061(4), Al−C(6) 2.010(4), W−C(1) 2.013(5), W−C(2) 2.002(5), W−C(3) 1.998(5), W−C(4) 2.005(5), W−C(5) 2.019(5); W−Al−N(1) 118.6(1), W−Al−N(2) 119.7(1), W−Al−C(6) 121.4-(2), N(1)−Al−C(6) 103.7(2), N(2)−Al−C(6) 101.8(2), Al−W−C(1) 88.2(1), Al−W−C(2) 88.1(2), Al−W−C(3) 177.1(1), Al−W−C(4) 80.8(2), Al−W−C(5) 87.2(2).

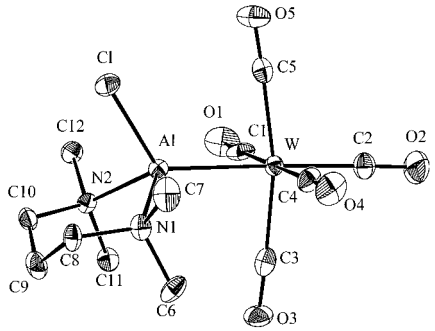

Figure 3. Molecular structure of $(CO)_5W-Al[(Cl)(TMPDA)]$ (**23**) in the crystal (ORTEP drawing; hydrogen atoms are omitted). Selected bond lengths (Å) and angles (deg): Al−W 2.645(2), Al−N(1) 2.074-(7), Al−N(2) 2.055(7), Al−Cl 2.199(3), W−C(1) 2.033(10), W−C(2) 2.007(8), W−C(3) 2.030(9), W−C(4) 2.028(9), W−C(5) 2.029(9); W−Al−N(1) 118.1(2), W−Al−N(2) 118.8(2), W−Al−Cl 124.2(1), N(1)−Al−N(2) 97.3 (3), N(1)−Al−Cl 96.2(2), N(2)−Al−Cl 96.5(2), Al−W−C(1) 90.9(2), Al−W−C(2) 175.9(3), Al−W−C(3) 86.2 (2), Al−W−C(4) 90.1(2), Al−W−C(5) 82.0(2).

D. Ab Initio Calculations. To achieve a better understanding of the bonding situation and the structural properties of the transition metal aluminum and gallium complexes reported in this work, we carried out quantum mechanical ab initio

(66) Weiss, J.; Fischer, R. A.; Pelletier, Y.; Reber, C. *Inorg. Chem.*, in press.

(67) Fischer, R. A.; Miehr, A.; Metzger, T. *Thin Solid Films* **1996**, *289*, 147−152.

(68) Barron, A. R.; Lyons, D.; Wilkinson, G.; Motevalli, M.; Howes, A. J.; Hursthouse, M. B. *J. Chem. Soc., Dalton Trans.* **1986**, 279−285.

(69) Barron, A. R.; Wilkinson, G.; Motevalli, M.; Hursthouse, M. B. *J. Chem. Soc., Dalton Trans.* **1987**, 837−846.

(70) Miehr, A.; Fischer, R. A.; Herdtweck, E. Unpublished results, 1996−97.

(71) Fischer, R. A.; T., P.; Scherer, W. *J. Organomet. Chem.* **1993**, *459*, 65−71.

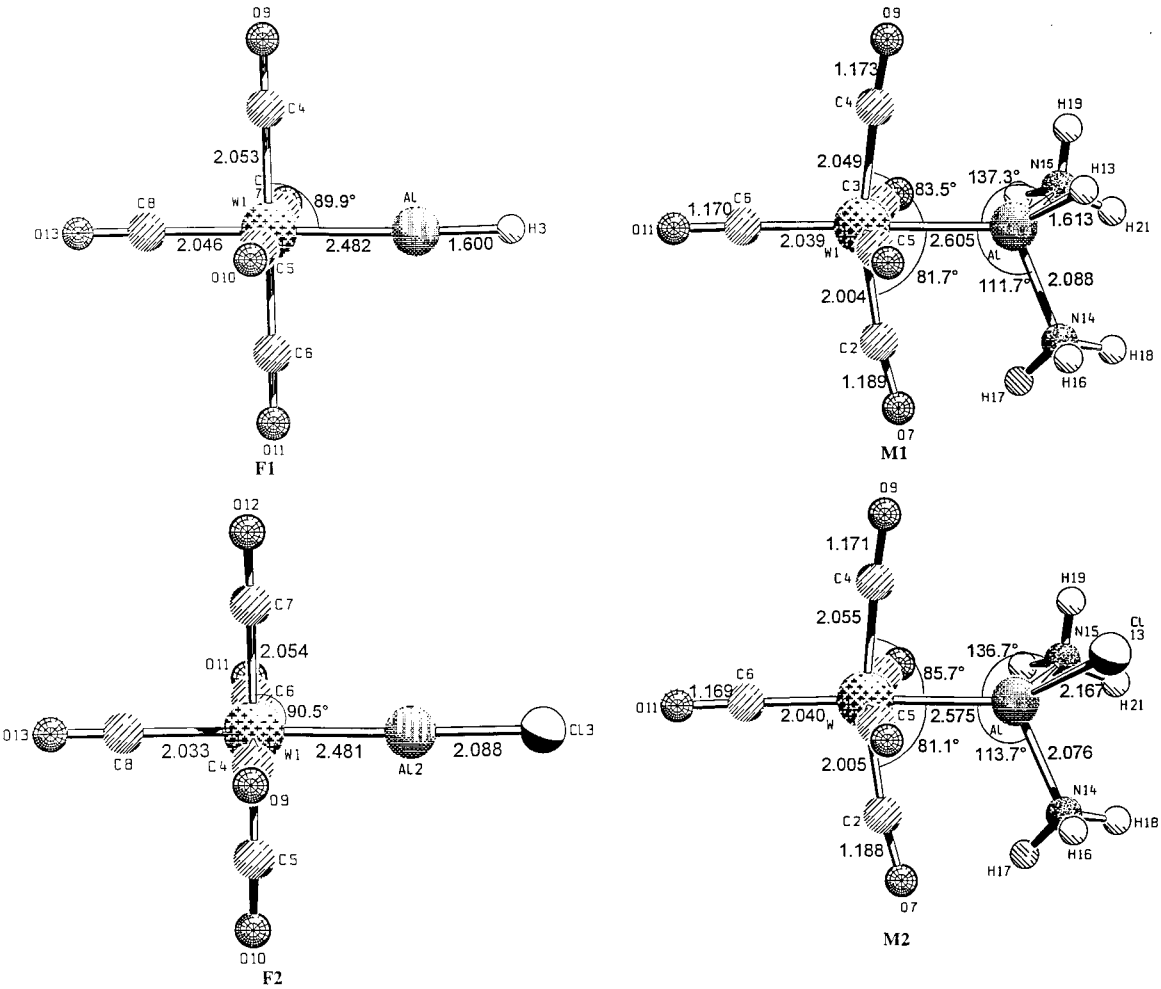

Figure 4. Calculated geometries at MP2/II. Bond lengths are given in angstroms and angles in degrees.

calculations at the MP2 level of theory for the model compounds (model = M) $(CO)_5W-Al[H(NH_3)_2]$ (**M1**), $(CO)_5W-Al[Cl(NH_3)_2]$ (**M2**), $(CO)_5W-Ga[Cl(NH_3)_2]$ (**M3**), $(CO)_5W-B[Cl(NH_3)_2]$ (**M4**), $(CO)_5W-In[Cl(NH_3)_2]$ (**M5**), and $(CO)_5W-Tl[Cl(NH_3)_2]$ (**M6**). The hydride complex **M1** was taken as the model for the alkyl-substituted species. To investigate the trend in the bond strength for $(CO)_5W-E[Cl(NH_3)_2]$, we calculated the whole series of complexes of the group-13 elements E = B−Tl. The complexes **M1** and **M2** are investigated theoretically in more detail by calculating the structures of the base free fragments $(CO)_5W-AlH$ (**F1**) and $(CO)_5W-AlCl$ (**F2**; fragment = F).

Figure 4 shows the optimized geometries of **M1** and **M2**, which have C_s symmetry. The theoretically predicted bond lengths of **M1** are in reasonable agreement with the experimental values of **20**. The calculated W−Al distance of **M1** (2.605 Å) is slightly shorter than the observed bond length of **20** (2.670 Å), while the theoretical Al−N distance of **M1** (2.088 Å) is conformable to the experimental values of **20** (2.061−2.0985 Å). The W−Al and the Al−N bonds of **M1** are clearly longer than the respective bonds of **M2** (W−Al, 2.575 Å; Al−N, 2.076 Å), which is in agreement with the bond shortening of the W−Ga and Ga−N bonds observed when the alkyl ligand in **6** and **7** is substituted by the chloro ligand (compound **2**). The calculations of **M1** and **M2** reproduce the umbrella effect of the $M(CO)_5$ fragment, which is found for the metallaalanes and -gallanes by X-ray structure analysis. The cis-CO groups of **M1** and **M2** are bent toward the $Al[R(NH_3)_2]$ (R = H, Cl) ligand between 81.1° and 85.7° (Figure 4).

Table 6. Calculated Dissociation Energies D_e and D_0 (Including ZPE[b] Contributions) at MP2/II

molecule	no.	symm	bond	D_e, kcal/mol	D_0,[b] kcal/mol
$(CO)_5WAlH(NH_3)_2$	**M1**	C_s	W−Al	100.9	97.9
			Al−N	64.0[a]	56.4[a]
$(CO)_5WAlCl(NH_3)_2$	**M2**	C_s	W−Al	93.1	86.2
			Al−N	65.2[a]	62.8[a]
$(CO)_5WAlH$	**F1**	C_{4v}	W−Al	70.0	68.1
$(CO)_5WAlCl$	**F2**	C_{4v}	W−Al	58.4	57.4
$AlH(NH_3)_2$		C_s	Al−N	33.1[a]	26.9[a]
$AlCl(NH_3)_2$		C_s	Al−N	30.5[a]	25.0[a]
$(CO)_5WGaCl(NH_3)_2$	**M3**	C_s	W−Ga	70.9	
$(CO)_5WBCl(NH_3)_2$	**M4**	C_s	W−B	119.6	
$(CO)_5WInCl(NH_3)_2$	**M5**	C_s	W−In	70.5	
$(CO)_5WTlCl(NH_3)_2$	**M6**	C_s	W−Tl	47.8	

[a] Dissociation energy of two NH_3 Ligands. [b] ZPE contributions are taken from HF/II calculations.

Table 6 shows that the calculated bond energies at the MP2/II level of theory for the W−Al bonds of **M1** and **M2** are D_e = 100.9 and 93.1 kcal/mol, respectively. At the same level of theory, the first dissociation energy of a CO ligand from $W(CO)_6$ is 54.9 kcal/mol, while the experimental value is 46.0 ± 2 kcal/mol.[72] Thus, the W−Al bonds of **M1** and **M2** are very strong. It is interesting to see that **M1** has a *stronger yet longer* W−Al bond than **M2**. This can be explained by the hybridization of the aluminum lone-pair donor orbital (Table 7). The Al electron

(72) Lewis, K. E.; Golden, D. M.; Smith, G. P. *J. Am. Chem. Soc.* **1984**, *106*, 6, 3905−3913.

Table 7. Results of the NBO Analysis at MP2/II: Partial Charges *q*, Wiberg Bond Indices *P*, Hybridization of the Lone-Pair Donor Orbital at Atom E[a] Given by the s Contribution (Occupancies in Parentheses)

molecule	no.	*q*(W)	*q*(W(CO)$_5$)	*q*(E)[a]	*P*(W−E)[a]	% s (lp)[a]
(CO)$_5$WAlH(NH$_3$)$_2$	**M1**	−0.67	−0.93	1.09	0.37	23.0 (0.824)
(CO)$_5$WAlCl(NH$_3$)$_2$	**M2**	−0.72	−0.90	1.24	0.40	23.9 (0.807)
(CO)$_5$WAlH	**F1**	−0.93	−0.64	1.07	0.60	62.5 (0.868)
(CO)$_5$WAlCl	**F2**	−0.94	−0.58	1.13	0.59	64.1 (0.824)
AlH(NH$_3$)$_2$				0.32		77.5 (1.94)
AlCl(NH$_3$)$_2$				0.54		84.0 (1.94)
AlH				0.60		91.5 (1.96)
AlCl				0.68		93.8 (1.95)
(CO)$_5$WGaCl(NH$_3$)$_2$	**M3**	−0.73	−0.72	1.07	0.44	18.3 (0.748)
(CO)$_5$WBCl(NH$_3$)$_2$	**M4**	−0.53	−0.63	0.19	0.42	35.2 (1.225)
(CO)$_5$WInCl(NH$_3$)$_2$	**M5**	−0.71	−0.77	1.18	0.42	19.8 (0.760)
(CO)$_5$WTlCl(NH$_3$)$_2$	**M6**	−0.70	−0.61	1.08	0.42	36.2 (0.908)

[a] E = Al, Ga, B, Tl, respectively.

lone pair of AlCl(NH$_3$)$_2$ has a higher s-character (84%) than that of AlH(NH$_3$)$_2$ (77.5%). A higher s-character makes the lone pair orbital more compact and more tightly bound. The latter leads to weaker donor−acceptor interaction, while at the same time the smaller size of the lone-pair orbital yields a shorter donor−acceptor bond. The lone-pair donor orbital at Al still has a slightly higher s-character in the complex **M2** (23.9%) than in **M1** (23.0%). However, the Al donor orbitals in the complexes **M1** and **M2** are occupied by only ∼0.8 electron (Table 7). There is significant electron donation from the Al-[R(NH$_3$)$_2$] donor to the W(CO)$_5$ acceptor in **M1** and **M2**. The charge donation to the W(CO)$_5$ moiety is 0.93 electron for **M1** and 0.90 electron for **M2**. The calculated charge donation and the strongly negative atomic charges at W (−0.67 in **M1**, −0.72 in **M2**) and positive charges at Al (+1.09 in **M1**, +1.24 in **M2**) indicate a substantial ionic character of the W−Al bond. This is further supported by the rather low Wiberg bond indices for the W−Al bonds (0.37 for **M1**, 0.40 for **M2**).

Base Free Complexes. Figure 4 also shows the optimized geometries of (CO)$_5$W−AlH (**F1**) and (CO)$_5$W−AlCl (**F2**). The most remarkable feature of the base free complexes are the nearly perfect octahedral structures, which *do not* exhibit the umbrella effect of **M1** and **M2**. It follows that the bending of the cis-CO ligands toward aluminum in **M1** and **M2** cannot be due to W → Al back-bonding, because this will be more important in the base free complexes than in **M1** and **M2**. The W−Al bonds of **F1** and **F2** are significantly shorter than those of **M1** and **M2** (Figure 4), but interestingly the bond energies of the base free complexes are more than 30 kcal/mol *lower* than calculated for **M1** and **M2** (Table 6). Again, this can be explained by the hybridization of the Al lone-pair orbital in the donor fragment. Table 7 shows that the aluminum lone-pair orbitals of AlH and AlCl have a much higher percent s-character (91.5% and 93.8%, respectively) than those of AlH(NH$_3$)$_2$ and AlCl(NH$_3$)$_2$ (77.5% and 84%). Also the Al lone-pair donor orbitals in **F1** and **F2** have a much higher percent s-character than those of **M1** and **M2** (Table 7).

Another interesting aspect concerns the intraligand Al−Cl and Al−N bonds. The Al−Cl and Al−N bonds of the ligands become significantly shorter in the complexes **M1**, **M2**, **F1**, and **F2**. Table 6 shows that the Al−NH$_3$ bonds of **M1** and **M2** are clearly stronger (64.0 kcal/mol for two NH$_3$ in **M1**, 65.1 kcal/mol in **M2**) than in the free ligands AlH(NH$_3$)$_2$ (33.1 kcal/mol) and AlCl(NH$_3$)$_2$ (30.5 kcal/mol). This is due to the electron donation from the Al lone-pair orbital to the (CO)$_5$W fragment. The positive charge at Al is much higher in **M1** (+1.09) and **M2** (+1.24) than in AlH(NH$_3$)$_2$ (+0.32) and AlCl(NH$_3$)$_2$ (+0.54). The charge donation Al → W yields a more electron deficient aluminum atom, which becomes a better electron acceptor for NH$_3$ and a better π-acceptor for chlorine.

We investigated the W−Al bond of **M1** using the topolgical analysis of the electron density distribution developed by Bader.[15] Figure 5 shows the Laplacian distribution of the complexes **M1** and **F1** and of the donor ligands AlH(NH$_3$)$_2$ and AlH. We discuss the W−Al bonding in the complexes by a buildup procedure beginning with AlH. The Laplacian distribution of the diatomics shows clearly an area of electron concentration at the aluminum atom ($\nabla^2\rho(r) < 0$, solid lines) which represents the lone-pair electrons. The electron concentration at Al in (CO)$_5$WAlH becomes deformed and shifted toward the π-bonding region as the result of the W−Al bond formation.

The area of electron concentration at Al in the ligand AlH(NH$_3$)$_2$ is less sickle-shaped and becomes more halfmoon-shaped than in AlH (Figure 5). This is in agreement with the calculated hybridization of the Al lone-pair electrons, which have less percent s-character in the former ligand than in the base free species (Table 7). A comparison of the electron concentration in the W−Al bonding region of **M1** with the base free complex **F1** shows clearly that in **M1** the concentration is more in the π-bonding region along the W−Al bond path. The base free complex has a larger area of electron concentration in the area of the W−Al π-bonding, which suggests stronger W → Al back-donation in **F1** than in **M1**.

Additional information about the metal−ligand interactions is given by the results of the charge-decomposition analysis (CDA)[16] of the complexes which are given in Table 8. We emphasize that the calculated numbers for the ligand → metal donation and metal → ligand back-donation can be used to estimate the *relative* donor and acceptor strength of the ligands, while the *absolute* numbers have little meaning.[16,73] A recent comparative study of the metal−ligand interactions in M(CO)$_5$L (M = Cr, Mo, W) and M(CO)$_3$L (M = Ni, Pd, Pt) for several ligands L has shown that the CDA results are in general agreement with the standard classification suggested from the analysis of vibrational spectra and molecular geometries.[73c]

(73) (a) Frenking, G.; Pidun, U. *J. Chem. Soc., Dalton Trans.* **1997**, 1653−1662. (b) Pidun, U.; G. Frenking, G. *Organometallics* **1995**, *14*, 5325−5336. (c) Ehlers, A. W.; Dapprich, S.; Vyboishchikov, S. F.; Frenking, G. *Organometallics* **1996**, *15*, 105−117. (d) Dapprich, S.; Frenking, G. *Organometallics* **1996**, *15*, 4547−4551. (e) Pidun, U.; Frenking, G. *J. Organomet. Chem.* **1996**, *525*, 269−278. 1996. Frenking, G.; Dapprich, S.; Köhler, K. F.; Koch, W.; Collins, J. R. *Mol. Phys.* **1996**, *89*, 1245−1263.

(74) Mocker, M.; Robl, C.; Schnöckel, H. *Angew. Chem.* **1994**, *106*, 1860−1861; *Angew. Chem., Int. Ed. Engl.* **1994**, *33*, 1754−1755.

(75) Uhl, W.; Hiller, W.; Layh, M.; Schwarz, W. *Angew. Chem.* **1992**, *104*, 1378−1380; *Angew. Chem., Int. Ed. Engl.* **1992**, *31*, 1364−1366.

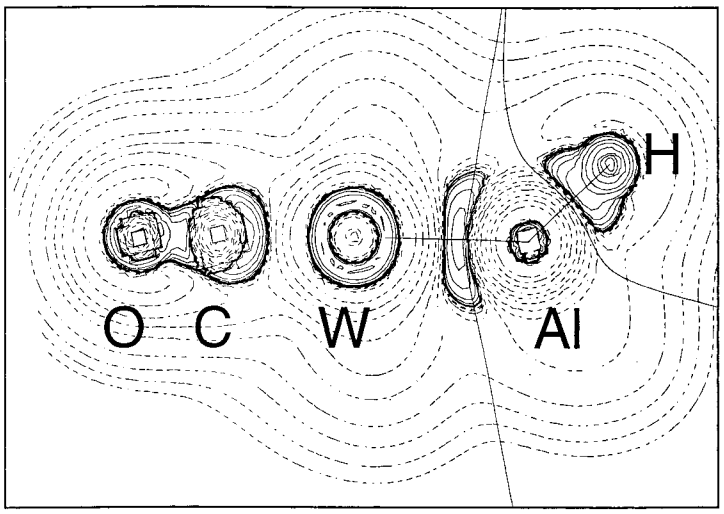

M1

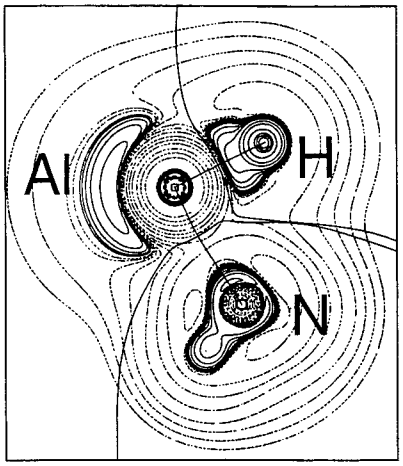

$Al[H(NH_3)_2]$

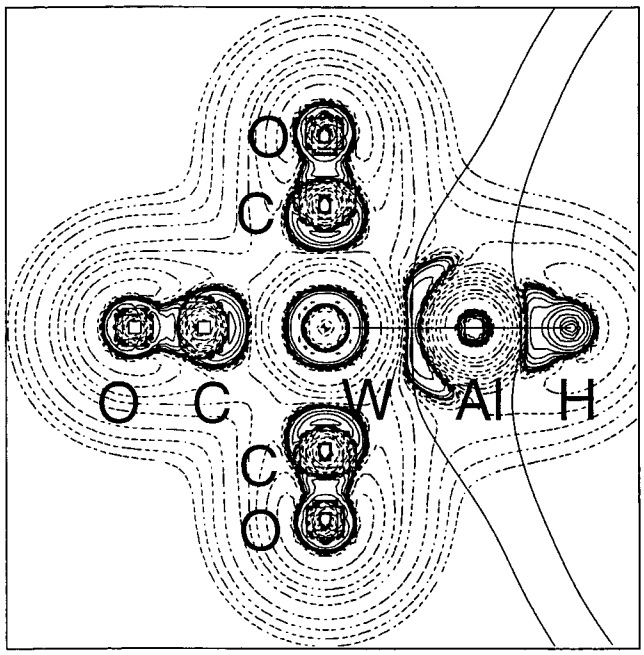

F1

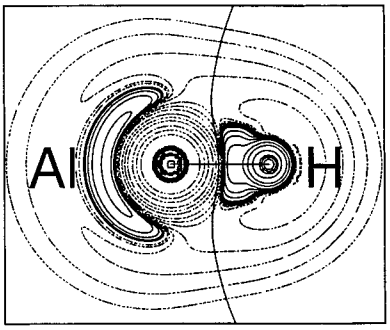

AlH

Figure 5. Contour line diagrams of the Laplacian distribution $\nabla^2\rho(r)$ at MP2/II of **M1**, **F1**, $Al[H(NH_3)_2]$, and AlH. Dashed lines indicate charge depletion ($\nabla^2\rho(r) > 0$); solid lines indicate charge concentration ($\nabla^2\rho(r) < 0$). The solid lines connecting the atomic nuclei are the bond paths; the solid lines separating the atomic nuclei indicate the zero-flux surfaces in the plane. The crossing points of the bond paths and zero-flux surfaces are the bond critical points r_b.

Table 8. CDA Results at MP2/II for the Metal−Ligand Donor−Acceptor Bonds: Ligand to Metal Donation M ← L, Back-Donation M → L, and Repulsive Polarization M ↔ L

molecule	no.	bond	donation M ← L	back-donation M → L	repulsion M ↔ L
$(CO)_5WAlH(NH_3)_2$	**M1**	W−Al	0.474	0.271	−0.353
		Al−N	0.643	0.069	−0.415
$(CO)_5WAlCl(NH_3)_2$	**M2**	W−Al	0.356	0.280	−0.290
		Al−N	0.679	0.056	−0.449
$(CO)_5WAlH$	**F1**	W−Al	0.399	0.301	−0.364
$(CO)_5WAlCl$	**F2**	W−Al	0.370	0.301	−0.260
$AlH(NH_3)_2$		Al−N	0.453	−0.019	−0.453
$AlCl(NH_3)_2$		Al−N	0.489	−0.009	−0.535
$(CO)_5WGaCl(NH_3)_2$	**M3**	W−Ga	0.434	0.213	−0.272
$(CO)_5WBCl(NH_3)_2$	**M4**	W−B	0.196	0.095	−0.428
$(CO)_5WInCl(NH_3)_2$	**M5**	W−In	0.449	0.207	−0.265
$(CO)_5WTlCl(NH_3)_2$	**M6**	W−Tl	0.411	0.114	−0.189

Table 8 shows that both ligands Al[R(NH$_3$)$_2$] and AlR (R = H, Cl) are strong donors, but also *significant acceptors*, as it was conjectured from the (CO) force constant analysis (see section C). The calculated donation and back-donation indicate that AlH and AlCl are stronger acceptors than Al[H(NH$_3$)$_2$] and Al[Cl(NH$_3$)$_2$], which is reasonable. The CDA results also show that NH$_3$ is a pure donor ligand in Al[R(NH$_3$)$_2$], **M1**, and **M2**. The calculated Al → N back-donation is negligible in comparison with the Al ← N donation (Table 8).

Now we compare the whole series of group-13 complexes (CO)$_5$W−E[Cl(NH$_3$)$_2$] for E = B−Tl. The W−E bond lengths increase from E = boron (2.349 Å) to E = thallium (2.800 Å). Note that the W−Ga bond (2.586 Å) is only slightly longer than the W−Al bond (2.575 Å). The trend of the (CO)$_5$W−E[Cl(NH$_3$)$_2$] bond dissociation energies is quite interesting. The strongest bond is calculated for E = B (D_e = 119.6 kcal/mol), and the weakest bond for E = Tl (D_e = 47.8 kcal/mol). The W−Al bond is also very strong (D_e = 93.1 kcal/mol). The W−Ga (D_e = 70.9 kcal/mol) and W−In (D_e = 70.5 kcal/mol) bonds have similar bond energies. It is a challenge to experiment that analogues of the complex with the theoretically predicted strongest W−E bond, i.e., (CO)$_5$WB[Cl(NH$_3$)$_2$], have not been synthesized so far, while the higher homologues (except Tl) are known. We attempted to synthesize (CO)$_5$W−B[Cl(tmeda)] (**25**). IR (CO) and ^{11}B NMR spectrosopic data obtained from reaction solutions suggest the presence of a species such as **25**. However, we have been unable to isolate boron complexes in a pure form, so far.

Conclusion

A series of new mixed metal complexes **1**−**24** were obtained by simple salt elimination employing carbonylmetalate dianions and XECl$_2$ (X = Cl, alkyl). On the basis of structural and spectroscopic data as well as ab initio quantum chemical calculations on some tungsten-group 13 element model complexes **M1**−**M6**, the M−E interaction was characterized as rather strong donor−acceptor bonds with significant ionic contributions. The hypothetic base free systems **F1** and **F2** as well as [(η^5-C$_5$H$_5$)Al−Fe(CO)$_4$][5a] exhibit much weaker M−E bonds than the Lewis base adducts **M1** and **M2**. This is due to a higher σ-character of the M−E bonding orbital rather than an effect of multiple bond π-interaction, which was calculated to be rather weak. The Lewis base ligands strongly increase the donor capacity of the whole fragment E(X)L$_2$ toward the Lewis acid (CO)$_5$M. The intraligand E−N donor−acceptor bonds are stronger in the complexes than in the free ligands. The structural analogy of the compounds **1**−**24** with complexes such as [(CO)$_5$Cr−InBr(THF)]$_n$,[39] {(CO)$_n$M−In[(3,5-Me$_2$-pz)$_3$BH]} (M = Fe, W; n = 4, 5; 3,5-Me$_2$pz = 3,5-dimethylpyrazolyl),[32] and {(CO)$_3$Ru[Ga(Cl)(thf)$_2$][Ga(Cl)$_2$(thf)]$_2$},[76] which had been formally classified by other authors as complexes containing In^{I} and Ga^{I} centers, suggests the description of the new compounds as Al^{I} and Ga^{I} systems. The assignment of formal oxidation numbers for atoms or functional groups in compounds strictly follows a self-consistent scheme based on the formal distribution of the valence electrons of the covalent bonds between atoms or groups of different electronegativities. The group electronegativity of a 16e fragment (CO)$_5$M can be estimated to be around 4−5,[77] similar to that of a fluoro or oxo ligand. Therefore, a description of the new complexes as Al^{III} and Ga^{III} systems is quite straightforward, but it would differ from the accepted practice in the literature (see above). Being aware that this issue is mostly a semantic one, we suggest at least two good reasons to indeed address compounds of the type (CO)$_n$M−E[(X)L$_2$] as Lewis base adducts of transition metal stabilized Al^{I} and Ga^{I} fragments. First, the reactivity of the new compounds is characteristically different from that of their E^{III} congeners: i.e., no M−E^{I} bond heterolysis in polar coordinating solvents and the splitting of the M−E^{I} bond upon treatment with appropriate neutral ligands (CO, bipy, ^{t}Bu-dab). Second, the exchange of a chloro ligand against an alkyl (or hydride) ligand at the Al or Ga center leads to *stronger* (but longer) bonds in contrast to the situation observed for the M−E^{III} systems.[78] The fragments E(X)L$_2$ behave as strong neutral 2e donating ligands and are isolobal to the well-known donor-stabilized silylenes and germylenes as well as to classical amine and phospine donor ligands. The heuristic value of this view is the following. It immediately leads to the idea to use the new compounds as an easily accessible synthetic equivalent or source for new Al^{I} and Ga^{I} chemistry, without being restricted to very special sterically overcrowded substituents as in the case of the complexes (CO)$_4$Fe−Al(η^5-C$_5$Me$_5$)[5a] or (CO)$_4$Fe−Ga(C$_6$H$_3$Mes*$_2$) (Mes* = 2,4,6-^{i}Pr$_3$C$_3$H$_2$).[5b]

Acknowledgment. We thank the Deutsche Forschungsgemeinschaft (Fi 502-2/4, Fr 641-4/1, SFB 260, and Graduiertenkolleg "Metallorganische Chemie") and the Fonds der Chemischen Industrie. Excellent service was provided by the computer centers HRZ Marburg, HLRZ Darmstadt, and HLRZ Jülich. S.F.V. thanks the DAAD for a scholarship. We also thank Professor Gütlich (Mainz) for Mössbauer spectroscopy of **12**.

Supporting Information Available: Full elemental analysis data for **1**−**24** and X-ray crystallographic files in CIF format for compounds **2**, **20**, and **23** are available in both hardcopy (21 pages) and electronic form. See any current masthead page for ordering and Internet access instructions.

JA9716463

(76) Harakas G. N.; Whittlesey, B. R. *Inorg. Chem.* **1997**, *36*, 2704−2707.

(77) Sen, K. D.; Böhm, M. C.; Schmidt, P. C. *Struct. Bonding* **1987**, *66*, 100−122.

(78) Frenking, G.; Böhme, C. Unpublished results, 1997.